ISPRS Journal of Photogrammetry and Remote Sensing 181 (2021) 295–307

Contents lists available at ScienceDirect

ISPRS Journal of Photogrammetry and Remote Sensing

journal homepage: www.elsevier.com/locate/isprsjprs

A comparison between TLS and UAS LiDAR to represent eucalypt crown fuel characteristics

Samuel Hillman [a,c,*], Luke Wallace [b], Karin Reinke [a,c], Simon Jones [a,c]

[a] School of Science, RMIT University, Melbourne, VIC 3001, Australia
[b] School of Geography and Environmental Studies, University of Tasmania, Hobart, TAS 7001, Australia
[c] Bushfire and Natural Hazards Cooperative Research Centre, East Melbourne, VIC 3004, Australia

ARTICLE INFO

Keywords:
UAS
Drone
LiDAR
3D remote sensing
TLS
Fuel

ABSTRACT

Advances in fire behaviour modelling provide a catalyst for the development of next generation fuel inputs. Fire simulations underpin risk and consequence mapping and inform decisions regarding ecological and social impacts of different fire regimes. Unoccupied Aerial Systems (UAS) carrying Light Detection and Ranging (LiDAR) sensors have been proposed as a source of structural information with potential for describing fine fuel properties. Whilst these systems have been shown to be capable of describing general vegetation distribution, the ability to distinguish between vegetation elements that contribute to fire spread and those that do not (such as large woody elements) is yet to be explored. This study evaluates the ability of UAS LiDAR point clouds to provide a description of crown fuel elements in eucalypt trees. This is achieved through comparison with dense Terrestrial Laser Scanning (TLS) that were manually attributed with a fuel description. Using the *TLSeparation* package TLS and UAS LiDAR point clouds achieved 84.6% and 81.1% overall accuracy respectively in the separation of crown fuel and wood in nine reference trees. When applying the same separation process across a 30 by 50 m plot consisting of approximately 75 trees, total canopy fuel volume was found to be strongly correlated between the TLS and UAS LiDAR point clouds (r: 0.96, RMSE: 1.53 m^3). A lower canopy base height and greater distance between crown fuel regions within each crown supported visual inspection of the point clouds that TLS point clouds were able to represent the crown to a greater extent than UAS LiDAR point clouds. Despite these differences it is likely that a less complete representation of canopy fuel such as that generated from UAS LiDAR point clouds will suitably represent the crown and canopy fuel objects effectively for fire behaviour modelling purposes. The research presented in this manuscript highlights the potential of TLS and UAS LiDAR point clouds to provide repeatable, accurate 3D characterisation of canopy fuel properties.

1. Introduction

Modelling fire behaviour assists land managers in understanding the potential rate of spread of fire and in-turn the potential impacts of fire on communities and ecosystems (Gazzard et al., 2020; Gorte and Economics, 2013; Penman and Cirulis, 2020). Given the importance of these models for decision making, it is imperative that core inputs of fuel, weather and topography are accurate and fit-for purpose (Sullivan et al., 2012). A description of fuel characteristics over the entire vegetation profile is necessary for accurate fire behaviour modelling. Canopy fuel inputs however are especially important due to the highly erratic and dangerous fire behaviour that is produced from crown fires with higher spread rate, fireline intensity, smoke production, spotting and turbulence (Cruz and Alexander, 2013). Maps of canopy fuel hazard are used in fire behaviour models around the world, especially in fire behaviour models developed for coniferous forests such as Nexus (Scott, 1999), Farsite and Flammap (Finney, 1998, 2006), Crown Fire Initiation and Spread(CFIS) (Van Wagner, 1977; Alexander et al., 2006). The characterisation of fine fuels is of particular importance due to these fuels being more responsive to dry weather and short-term changes in atmospheric variations in moisture conditions (Rothermel, 1986; Viney, 1991) and allowing fire to propagate faster with higher flame heights and intensity (Hines et al., 2010; Raymond and Peterson, 2005).

The definition outlined in Cruz et al. (2004) when describing aerial fuels is applied in this research where 'crown' is applied to describe aerial fuels at the tree level and 'canopy' at the stand level. Several

* Corresponding author at: School of Science, RMIT University, Melbourne, VIC 3001, Australia.
E-mail addresses: samuel.c.hillman@gmail.com, samuel.hillman@student.rmit.edu.au (S. Hillman).

https://doi.org/10.1016/j.isprsjprs.2021.09.008
Received 3 April 2021; Received in revised form 7 September 2021; Accepted 8 September 2021
Available online 30 September 2021

metrics have been used to describe canopy properties; Canopy Fuel Load (CFL) also referred to as Canopy Fuel Weight (CFW), Canopy Bulk Density (CBD) and Canopy Base Height (CBH) (Mitsopoulos and Dimitrakopoulos, 2007; Cruz et al., 2004). These metrics have been developed and assessed using a combination of destructive harvesting techniques, visual based assessments, and species-specific regression models using standard forest biometric measurements such as tree density, mean height and Diameter at Breast Height (DBH) (Skowronski et al., 2011; Duveneck and Patterson, 2007; Keane, 1998; Keane et al., 2000). These metrics have largely been developed in coniferous forests with little work conducted in mixed forests with non-homogenous (heterogeneous) canopies (Gould et al., 2008; Cruz et al., 2013).

Developments in remote sensing technologies, in particular Light Detection and Ranging (LiDAR) sensing systems, present pathways to empirically measure and analyse vegetation structure at scales appropriate for fire behaviour modelling. Terrestrial Laser Scanners (TLS) have been shown to be able to accurately calculate biomass, characterise stem properties, develop allometric biomass relationships and observe fine scale vegetation characteristics (Disney et al., 2019; Newnham et al., 2015; Calders et al., 2015; Rowell et al., 2016). TLS point clouds have also been utilised to estimate canopy attributes of height and cover (Hillman et al., 2021; García et al., 2011; Danson et al., 2014). Strong correlation of TLS derived attributes to field measurements for crown base height, crown diameter and crown volume have been observed in deciduous stands (García et al., 2011). High density point cloud information produced from TLS scans allows novel classification methods to be developed (Hillman et al., 2021; Chen et al., 2016).

An area which has been the focus of recent investigation has been the separation of leaf and wood material using TLS point clouds (Ma et al., 2015; Zhu et al., 2018; Wang et al., 2018, 2020). Methods used to separate points into the respective leaf and wood classes can be grouped into methods which utilise the intensity of returned points, geometry (location and proximity of points) or a mixture of both (Vicari et al., 2019). Intensity based methods separate the components of the tree based on the different optical properties at the operating wavelength of the laser scanner (Béland et al., 2014; Wang, 2020). Limitations with intensity-based separation methods have been highlighted in dense canopies where partial reflectances can generate misleading intensity values in addition to the need for the scanner to be calibrated to generate accurate separation (Tao et al., 2015a). Geometry based methods for separating components of the tree require only the 3D coordinates of points and have shown to be effective at separating leaf and wood material whilst also being less labour and time intensive than supervised classifiers (Tao et al., 2015a; Ma et al., 2015; Zhu et al., 2018; Wang et al., 2020; Krishna et al., 2019; Vicari et al., 2019; Wang et al., 2020). The development of these algorithms has largely been focused in single-layered forests, coniferous and/or broadleaved trees which largely have a uniform structure (Hall et al., 2005; Wulder and Seemann, 2003; Patenaude et al., 2005). A current gap in the literature exists in the trial of leaf and wood separation algorithms in eucalypt forests. The crowns in eucalypt systems are distinct to coniferous forests with mostly woody, sclerophyllous and evergreen trees with highly variable crowns that have small, rigid leaves which are also erectophile in orientation in response to the high sun intensity (Lee and Lucas, 2007). Due to different structure of the crowns, the applicability of the existing segmentation workflows needs to be verified and potentially optimised for their use in the separation of crown fuel in eucalypt systems. It is predicted that an automated approach to the classification of fine fuels in the canopy would allow for the determination of canopy fuel loads which are not currently utilised in Eucalypt fire behaviour models. That is, the separation of crown fuel provides an avenue for fire behaviour modellers to access information on the total volume and distribution of fuel across the crown.

Airborne LiDAR has been used extensively in northern hemisphere forests to estimate canopy fuel properties (Skowronski et al., 2007; Andersen et al., 2005; Hermosilla et al., 2014; González-Olabarria et al., 2012; Romero Ramirez et al., 2018; Engelstad et al., 2019; Zhao et al., 2011; Skowronski et al., 2011). In contrast mixed-forests have had limited research to determine canopy fuel properties from LiDAR (Cao et al., 2014; Latifi et al., 2016; Botequim et al., 2019; Guerra-Hernández et al., 2016). Promising studies in mixed-forests have reported medium to high correlations of field estimated stand height to LiDAR derived measurements, CFL, CBD and CBH (Botequim et al., 2019). Whilst airborne LiDAR provides wide area observations, this comes at the trade-off of lower point density and potentially greater cost depending on the size of data acquisition. UAS LiDAR is a bridging technology that trades off capturing smaller areas for more information describing vegetation beneath the canopy (Wallace et al., 2012; Wallace et al., 2016; Sankey et al., 2017; Guo et al., 2017; Cao et al., 2019). Previous UAS LiDAR (low-altitude) studies have predominantly focused on replicating existing metrics from fixed-wing airborne (high altitude) derived point clouds (Liu et al., 2018). Studies extracting canopy and tree-based volume and DBH metrics from UAS LiDAR point clouds have shown strong correlation to TLS point clouds and field-based estimates (Brede et al., 2017; Brede et al., 2019; Fritz et al., 2013; Wieser et al., 2017; Hillman et al., 2021; Wallace et al., 2014b,a; Peng et al., 2020). Whilst UAS LiDAR has been shown to be able to represent below canopy structure, limited research has been conducted in the ability of UAS LiDAR to measure fine-scale features such as leaves and fine twigs either below or at the canopy. It is predicted that with the different sampling geometry from UAS LiDAR in comparison to TLS, that stems are likely to be less continuous stems and have a lower relative precision (Levick et al., 2021).

The aim of this study is to investigate the capability for the method outlined in Vicari et al. (2019) to be utilised in the separation of crown fuel and wood in a eucalypt forest using data captured by TLS and UAS LiDAR. Secondary to this aim, a comparison between the TLS and UAS LiDAR point clouds in their ability to represent crown fuels will be conducted using manually separated reference trees and automatically classified point clouds (where TLS point clouds are considered to provide the best representation of vegetation). The distribution of canopy volume estimates are subsequently compared between UAS LiDAR and TLS calculated over a plot area of 30 $\times$ 50 m (1500 m^2). If shown to be successful in eucalypt forests, such an approach allows land managers to fully utilise high resolution 3D data and develop canopy fuel inputs for use in next generation fire behaviour models that accurately characterise the fuel objects.

2. Materials and methods

2.1. Study site

The study area consisted of two plots located south-east of Hobart in Ridgeway Tasmania, Australia. The first plot (T_1) consisted of a group of 9 trees that were located next to each other in a (25 $\times$ 30 m area). This set of nine trees were selected to provide a diverse array of tree heights, crown overlap and structure. The second plot (T_2) was a 30 $\times$ 50 m plot captured approximately 10 m from the isolated trees. The predominant forest type was native dry sclerophyll eucalypt forest (Fig. 1). The dominant canopy species consisted of *Eucalyptus pulchella* trees of mixed ages and ranging in height from 4.7 m to 16.2 m. Trees were distributed unevenly throughout the plot ranging from individually isolated trees, through to multiple trees with overlapping canopies. The study area had been subject to planned burning activities in 2016 which subsequently affected the distribution of leaf/fine fuel on the trees. For example, some trees had epicormic growth at the bottom of the stem with full leaf removal in the upper branches.

2.2. Terrestrial laser scanning data

TLS data was captured using a Trimble TX8 laser scanner (Trimble Inc., Sunnyvale, CA, USA) set to capture Level 2 quality scans (11.3 mm

Fig. 1. a) The location of the site in Tasmania, Australia b) Location of the site in Ridgeway, Tasmania; c) Photograph showing the dry eucalyptus forest in which the technology was assessed.

point spacing at a distance of 30 m). Two separate sets of scans were collected in line with the two separate plots (T_1, T_2). Capturing T_1 involved nine scans approximately 10 m apart and surrounding the trees (Fig. 2). The second plot (T_2) consisted of 24 scans which were captured in a 10 m grid pattern to allow full coverage of the plot (Fig. 2). The point density of the TLS scans were approximately 950,000 points/m^2.

TLS Scans were co-registered in Trimble Realworks 10.1 using scan-to-scan matching. The quality of the matches was assessed with scans manually adjusted through the use of common features found within the point cloud. To georegister the TLS data the same approach as discussed in Hillman et al. (2021) was implemented using a minimum of six common features (such as tree stems and stumps) that were identified in the geo-rectified UAS LiDAR point clouds and the relevant translation and rotation applied to the TLS point cloud. Visual inspection of the point clouds was then conducted to ensure accurate co-registration (to within 0.10 m).

2.3. UAS LiDAR data capture

LiDAR data was captured with a custom-built UAS developed at the University of Tasmania, Australia. The system consisted of a DJI M600 platform, a Velodyne Puck (VLP-16) and an Advanced Navigation Spatial Dual coupled GNSS and IMU sensor. The scanner and associated settings were the same as in Hillman et al. (2021). The scan angle was limited to −40° to +40° in the across-track direction (80° field-of-view) and across-track beam divergence of 0.18° (3.0 mrad); along-track: 0.07° (1.2 mrad), resulting in a laser footprint of 12.6 cm by 4.9 cm on the ground. Flight lines are illustrated in (Fig. 2). Flying height was 40 m above the ground level, with flight lines chosen to achieve approximately 50% overlap at ground level. Georeferenced LiDAR point clouds were generated using Python software code that was developed in-house specifically for UAS LiDAR processing (du Toit et al., 2020; Grubinger et al., 2020; Camarretta et al., 2020). Both T_1 and T_2 were captured in a single flight and resulted in a point density of approximately 330 points/m^2.

2.4. Point cloud preparation

Noise filtering to remove spurious points from both the TLS and UAS LiDAR point clouds was completed by manually inspecting and

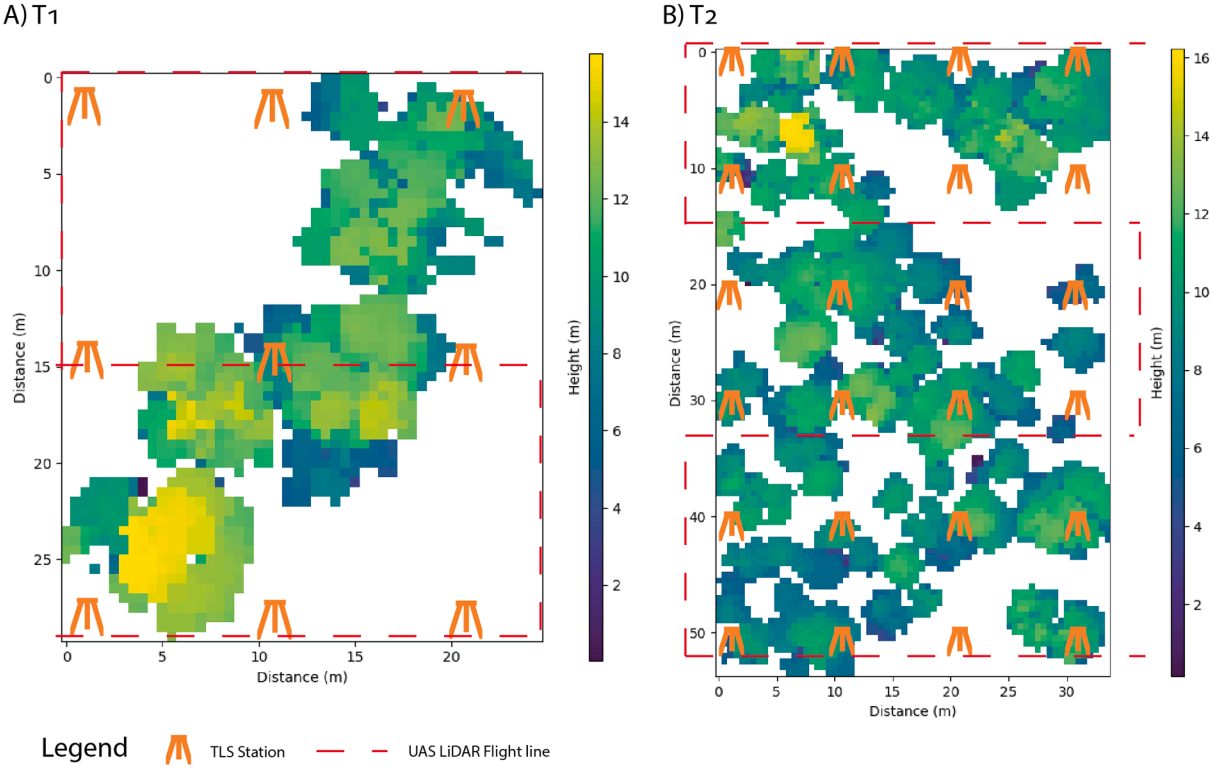

Fig. 2. a) Diagram of scan arrangement and flight lines for isolated group of trees (T_1); b) Plot diagram showing the distribution of TLS scans in T_2 with canopies shown and flight lines of UAS LiDAR capture.

removing points that were beneath the ground or several metres above the canopy. Subsequently a raster pouring approach as outlined in Hillman et al. (2021) was completed. This is a novel approach which considers the connections between voxel layers and allows vegetation objects to be allocated to a fuel strata in which they started. For this study, although there are no fixed height thresholds defined in the literature for describing fuel strata in dry eucalypt forests, we applied an approach consistent with fuel studies in eucalypt forests. This created four classes which capture the surface and near-surface combined fuel layer (<0.6 m), elevated (0.6 m to 3 m), intermediate (3 m-5 m) and canopy (>5 m) fuel layers(Hines et al., 2010; Gould et al., 2008). This process was applied on all point clouds to separate those points which describe the stem and crown elements from the elevated and near-surface and surface elements of the fuel strata.

In order to use the automatic leaf and wood separation algorithm outlined below each individual tree needed to be segmented into separate point clouds. In this case manual segmentation based on visual interpretation (using both point location and intensity) was considered to be the most likely to provide similar accuracy between the two point cloud sources (TLS and UAS LiDAR). This was completed in CloudCompare v2.12 (Girardeau-Montaut, 2016). Each tree from the UAS LiDAR point cloud was individually co-aligned to the respective TLS point cloud based on stem and branch matching. This process ensured high accuracy of co-alignment and accounted for any environmental effects (such as wind which was 0 to 5 km h^{-1}) effecting the tree alignment. Once aligned, all point clouds (TLS and UAS LiDAR) were normalised in density using a 0.02 m voxel size. This allowed efficient processing of the TLS data while allowing fine fuels to be represented and had negligible effect on the UAS LiDAR point clouds.

2.5. Crown fuel classification

2.5.1. Manual data labelling

The nine trees from T_1 were selected to generate attributed reference data. For each of the trees in T_1, the TLS point cloud of the tree was visually inspected with points manually labelled as originating from a woody component (greater than approx. 0.05 m) or from a crown fuel element (less than approx. 0.05 m). This process was completed in CloudCompare v2.12 (Girardeau-Montaut, 2016) utilising both geometry and intensity of point returns to assist the interpreter in separating the points. TLS point clouds were considered to provide the best representation of vegetation information and as such were used to develop the reference separation for the UAS point clouds of trees in T_1. For each tree in T_1, the class of the closest point in the classified TLS point cloud was assigned to each point in UAS point cloud.

2.5.2. Automated classification of crown fuels

Automated classification of crown fuels was conducted using the approach outlined in Vicari et al. (2019). The package *TLSeparation* (Vicari, 2017) is flexible in it's application and a bespoke workflow was created for the application in eucalypt forests for both the TLS and UAS point clouds. The workflow for extracting crown fuel and wood vegetation elements from TLS and UAS LiDAR point clouds was completed using distinct processing workflows. For a full description of the methods utilised in this manuscript, Vicari et al. (2019) outlines the workflow in more detail. Briefly, the algorithms that were used in the separation of points in this manuscript are a combination of path analysis and point-wise classification processes. For the path analysis, the point clouds are converted into a network graph where every point is represented by a node and connections between pairs of neighbouring points are represented by edges. Once the graph is made, path retracing and path frequency detection algorithms can be applied to identify the trunk and branches. For point-wise classifications, the geometry of each point is defined by calculating the eigenvalues (which can express data variability over orthogonally projected axes) of 3D coordinates using local subsets of points around it (Vicari et al., 2019). Features are then calculated using the normalised eigen values based on the features calculated and proposed by Ma et al. (2015), Wang et al. (2014). These features are then used to generate distribution models using Gaussian Mixture Model, which when coupled with Expectation/Maximization (EM) algorithms, are able to classify the features into a predefined number of classes (Vicari et al., 2019). In all cases the leaf points are determined by the difference between the identified wood points and initial point clouds.

For TLS point clouds, the *generic tree* workflow as described in the *TLSeparation* package (Vicari, 2017) was utilised with an optimised set of k nearest neighbours and voxel size to generate an initial separation of crown fuel and wood points. Based on visual inspection of the point clouds, a majority filter, continuity filter, and voxel path detection filter were subsequently applied to remove mis-classified points and establish a final separation of crown fuel and wood points. For the UAS LiDAR point clouds, the separation of crown fuel and wood points was completed using the inbuilt workflow *large tree 3* described in the *TLSeparation* package (Vicari, 2017). After completing the *large tree 3* automated tree algorithm, a majority filter was run to remove mis-classified points by comparing each point against its neighbours' classes.

2.5.3. Optimisation of automated classification parameters

Three representative trees from the TLS and UAS LiDAR point clouds were used as training trees to optimise the selection of parameters used in the respective workflows. The training trees were selected to represent a diversity of structural arrangements and heights. The parameters were selected for each algorithm by iterating over a set of possible combinations for the variables used in the respective workflows. For TLS point clouds these were k nearest neighbours(knn), voxel size, and search radius for filters (Table 1). For UAS LiDAR point clouds these were k nearest neighbours, voxel size and search radius for majority filter (Table 1). Parameters which resulted in the highest Matthews Correlation Coefficient (MCC) score for the separation of crown fuel and wood points across all three trees were selected for use in the final model. The MCC formula is defined as follows Eq. (1) where TP is the number of true positives, TN the number of true negatives, FP the number of false positives and FN the number of false negatives.

$$MCC = \frac{TP \times TN - FP \times FN}{\sqrt{(TP + FP)(TP + FN)(TN + FP)(TN + FN)}} \quad (1)$$

MCC was also utilised to provide a measure of classification accuracy of the nine reference trees. MCC has previously been applied in the analysis of point clouds (Gawel et al., 2016; Aijazi et al., 2013; Hillman et al., 2019) to compare observed and predicted binary classifications where the classes are imbalanced (Boughorbel et al., 2017).

Table 1
Optimised settings applied to TLS and UAS LiDAR point clouds to be used with *TLSeparation* (Vicari, 2017).

Filter Settings	TLS Settings	UAS LiDAR Settings
Automated separation algorithm	Generic tree	Large Tree 3
Automated separation algorithm - voxel size	0.02 m	0.02 m
Automated separation algorithm-nearest neighbours	20, 40, 60, 80, 100	20, 40, 60, 80, 120
Majority filter- search radius	0.05 m	0.05 m
Majority filter - number of nearest neighbours	100	40
Continuity filter-search radius	0.05 m	
Voxel path detection-voxel size	0.05 m	0.1 m
Voxel path detection-number of steps to retrace	4	varies depending on process (refer Vicari (2017) for more details)
Voxel path detection-number of nearest neighbours to fill in gaps	100	100
Voxel path detection-neighbour distance threshold	0.05 m	0.15 m

2.6. Crown volume, crown distance and canopy base height calculations

Once the crown fuel points were separated from wood points, the volume of the crown fuel points were calculated. To calculate volume, the alpha shapes algorithm was utilised to allow for the shape of a set of unorganized points to be described (Edelsbrunner and Mücke, 1994). The shape described by this algorithm is determined by the set of points and the value of alpha. Different alpha values were applied to TLS and UAS LiDAR point clouds. Visual inspection of the TLS point clouds was used to assess the resultant output shapes for how well they formed realistic crown fuel clumps (ie formed separate clumps and that contained minimal holes within clumps) and subsequently to identify the most suitable alpha value. In this case, alpha was set to 0.05 m for the TLS point clouds. For the UAS LiDAR point clouds, the alpha value 0.15 m was selected through minimising the RMSE of the crown volume when comparing the UAS LIDAR reference tree dataset with the TLS reference tree dataset.

Once the alpha shapes were created for each tree, a calculation to determine the shortest distance between each group or clump of alpha shapes for the tree was made. This calculation was made to investigate the differences in the ability of each technology to describe connections between crown fuel. Whilst not able to be currently used in fire behaviour models, this metric is one which is considered to be useful for describing the highly distributed nature of crown fuel elements in eucalypt trees. To calculate the distance, the euclidean distance between the nearest vertex of each shape was made to the neighbouring shapes. An average distance between regions was calculated for each tree.

Canopy base height (CBH) was calculated across the plot by firstly separating crown fuel points from each tree. Based on visual inspection of the point clouds and point distribution, the 10th percentile height of the crown points was then extracted to represent the Crown Base Height (CrBH) which ensured that outlying points did not have a large influence on results. A plot scale measurement of canopy cover, mean CBH and 90th percentile height (CTH) were derived from a 0.5 m grid size. The CTH is an input into fire behaviour models (Cruz et al., 2013; Scott, 2005) and is an important variable to demonstrates differences in the ability of each sensor to represent crown fuel elements at the top of trees.

2.7. Comparison of TLS and UAS LiDAR derived crown fuels

2.7.1. Classification assessment

Overall accuracy of classification was determined by using six of the nine trees extracted as reference trees (ie excluding trees that were used for parameter optimisation). An accuracy score was calculated from the confusion matrix for the classification of wood and crown fuel points. Due to the higher number of crown fuel points in comparison to wood points, MCC was utilised to provide a measure of classification accuracy of the nine reference trees. Errors of omission and commission of the respective crown fuel and wood points was also calculated for each reference tree.

2.7.2. Metric analysis

For the six reference trees in T_1 that were not used in the parameter optimisation, comparisons were conducted on the volume of crown fuels, distance between crown fuel elements and CrBH derived from reference and automated separation processes. Pearsons correlation coefficient, Root Mean Square Error (RMSE), mean and standard deviation were calculated for each respective metric and technology. This assessment gave an indication of the success of wood and crown fuel separation that could be considered when interpreting the results across a larger area in plot T_2.

Differences between the representation of canopy fuels by each technology at the plot level were investigated through comparing metrics (volume, distance between clumps and CBH) using Pearsons correlation coefficient, RMSE, Mean Bias Error (MBE), where TLS was assumed to provide the most accurate separation of canopy fuels. Statistical differences between CBH and CTH were analysed using a Wilcoxon signed-rank test (as CBH was found to be non-normally distributed) and a paired t-test respectively. Both tests were performed at the significance level of $\alpha 0.05$.

3. Results

3.1. Validation and training accuracy in T_1

For the six of the nine trees selected for the reference calculations in T_1 that were not used for parameter optimisation, automated classification of TLS point clouds had an average overall accuracy of 84.6% with overall accuracies for individual reference trees ranging from 72.8% to 95.0% (Table 2). UAS LiDAR point clouds had an average overall accuracy of 81.1% with overall accuracies for individual reference trees ranging from 51.5% to 95.1% (Table 3).

Whilst the overall accuracy results are similar between the TLS and UAS LiDAR point clouds, the MCC scores highlight differences in the accuracy of classification (Fig. 3). The TLS point clouds had MCC scores ranging from 0.45 to 0.84 with an average overall MCC score of 0.63 (excluding training trees), indicating moderate correlation between automated separation algorithms and reference separation. The highest MCC (0.84) was seen in tree 2 which had low errors of omission of crown fuel and wood (<6%) and low errors of omission of wood points (<5%). In trees (trees 4 and 6) that had lower MCC results (MCC <0.50), high errors of omission for crown fuel points (>25%) and commission in wood points were observed.

The MCC scores in UAS LiDAR point clouds were lower in comparison to TLS point clouds with an overall MCC average of 0.46 (Fig. 3). Similar to the TLS point clouds, the highest MCC in UAS LiDAR point clouds (0.76) was seen in tree 2. In contrast to TLS point clouds, trees extracted from the UAS LiDAR point clouds which had lower MCC results (MCC < 0.50) had higher errors of omission of wood points. This indicates that a large proportion of wood points are being misclassified. Of particular note is tree 6 which had a negative MCC value indicating that the automated separation was not successful on this point cloud.

3.2. Volume, distance, and CrBH comparison of reference trees in T_1

Strong correlation of crown volume estimates ($r > 0.97$) were found between reference trees and automated separation in the TLS and UAS LiDAR point clouds (Fig. 4). The TLS point clouds had a lower RMSE of 1.14 m^3, in comparison to UAS LIDAR point clouds 1.34 m^3. The mean volume of crown fuel points derived from the automatic separation for the TLS point clouds (5.57 m^3) was lower than the reference volume (6.13 m^3). In contrast the mean volume of crown fuel points derived from the automatic separation in UAS LiDAR point clouds (7.83 m^3) was higher than the reference volume (6.65 m^3).

Similar to crown volume estimates, there was strong correlation ($r > 0.96$) observed between reference trees and automated separation of the CrBH in both the TLS and UAS LiDAR point clouds. The mean CrBH in the TLS reference (6.19 m) and automated (6.51 m) separation point clouds was lower than the UAS LiDAR point clouds (automated: 7.34 m). Visual inspection of the point clouds (Fig. 5) confirmed the lower canopy elements were more consistently represented in the TLS point clouds compared to UAS LiDAR point clouds, where points representing lower crown elements were not always present.

The distance between clumps of crown points in the TLS point clouds was highly correlated (r: 0.68) between the reference and automated separation. Lower correlation (r: 0.48) and a greater RMSE of 0.71 m was observed between the distance between clumps of crown points in the reference and automated UAS LiDAR point clouds. In both the automated (3.33 m) and reference separation (2.92 m), the TLS point clouds recorded a greater distance between clumps in comparison to the UAS LiDAR point clouds (automated: 3.04 m). Visual inspection of the point clouds indicated that the TLS points clouds were able to form

Table 2
Summary of the number of voxels classified as crown fuel or wood from the reference trees, overall accuracy, MCC, and errors of omission (Omm) and commission (Comm) for the automated separation of crown fuel and wood points for TLS point clouds. (*Trees not included in calculations).

Tree	Voxel Count		Overall Accuracy (%)	MCC	Crown Fuel		Wood	
	Crown	Wood			Omm (%)	Comm (%)	Omm (%)	Comm (%)
Tree 1	232,601	59,325	90.4	0.75	9.90	2.27	8.20	29.71
Tree 2	843,465	165,038	95.0	0.84	5.07	1.01	4.95	21.41
Tree 3*	1,223,939	306,768	88.9	0.67	8.23	5.82	22.61	29.80
Tree 4	957,923	215,225	72.8	0.45	30.59	3.77	12.12	60.77
Tree 5	155,915	42,280	93.1	0.79	3.44	5.27	19.81	13.68
Tree 6	193,519	72,529	73.9	0.45	27.34	10.52	22.79	48.58
Tree 7	481,401	150,904	82.2	0.53	14.00	9.88	30.07	38.98
Tree 8*	1,062,163	197,529	80.4	0.38	15.55	8.30	41.12	58.68
Tree 9*	1,437,316	273,735	87.7	0.59	9.56	5.30	26.58	40.60
Average			84.6	0.63	15.06	5.45	16.32	35.52

Table 3
Summary of the number of voxels classified as crown fuel or wood from the reference trees, overall accuracy, MCC, and errors of omission (Omm) and commission (Comm) for the automated separation of crown fuel and wood points for UAS LiDAR point clouds. (*Trees not included in calculations).

Tree	Voxel Count		Overall Accuracy (%)	MCC	Crown Fuel		Wood	
	Crown	Wood			Omm (%)	Comm (%)	Omm (%)	Comm (%)
Tree 1	9,013	3,098	89.0	0.70	1.89	11.60	37.44	8.06
Tree 2	46,486	6,837	95.1	0.76	0.62	4.78	33.90	6.03
Tree 3*	42,481	7,787	88.1	0.45	1.93	10.99	66.62	24.09
Tree 4	27,168	5,198	89.7	0.56	0.58	10.52	61.06	7.20
Tree 5	3,239	1,022	80.9	0.42	7.26	16.14	56.56	34.61
Tree 6	4,336	3,470	51.5	−0.06	18.59	45.77	85.85	62.14
Tree 7	11,794	4,214	79.5	0.40	1.56	21.08	73.61	14.20
Tree 8*	13,420	2,588	87.4	0.43	0.95	12.47	73.18	15.57
Tree 9*	56,048	6,028	92.7	0.49	1.08	6.66	65.66	22.59
Average			81.1	0.46	5.08	18.31	58.07	22.04

tighter, more discrete clumps compared to UAS LiDAR.

3.3. Volume, distance, and CBH comparison at the plot scale (T_2)

A comparison of plot canopy volumes highlighted strong correlation (r: 0.96, RMSE: 1.53 m^3) between volumes derived from TLS and UAS LiDAR point clouds (Figs. 6 and 7). The total volume of canopy fuel at the site was lower in the TLS point clouds (332.09 $m^{3)}$ in comparison to the UAS LiDAR point clouds (365.75 m^3). The average crown volumes derived for each technology also show that UAS LiDAR point clouds had a greater average volume at the tree level (5.08 m^3) in comparison to TLS point clouds (4.61 m^3). This finding was supported by a mean bias error of −0.47 m^3 indicating that UAS LiDAR point clouds over-predict the volume of crown fuels.

Analysis of the average distance between clumps of crown fuel between the TLS and UAS LiDAR point clouds showed a correlation of r: 0.54 with an RMSE of 1.37 m (Fig. 6) at the plot scale. Additionally, TLS point clouds were shown to have greater distances between clumps evident through a positive MBE of 1.08 m. This was also reflected when the distance between clumps was averaged across the plot with a higher mean distance of 2.83 m in TLS point clouds in comparison to 1.75 m in UAS LiDAR point clouds. This suggests that the UAS LiDAR point clouds were detecting fewer clumps with smaller distances between each clump.

The canopy coverage across the plot was similar between each technology (TLS: 55.5% and UAS LiDAR 54.8%). There was a strong correlation (r: 0.79) between TLS and UAS LiDAR estimates of CBH (Fig. 8). The mean CBH was higher in the UAS point clouds when compared to the TLS point clouds indicating less penetration through the canopy which was also reflected in the mean bias error of −1.31 m. Examination of the p-value derived from the Wilcoxon signed-rank test highlighted that the null hypothesis should be rejected with the estimates of CBH between TLS and UAS LiDAR crown fuel points being statistically different (p-value: 9.46 e-13). Similarly, the CTH p-value derived from the paired t-test showed that the null hypothesis should be rejected with estimates of CTH between TLS and UAS LiDAR point clouds being statistically different (p-value: 8.13 e-16) with a higher mean height being observed in the UAS LiDAR points suggesting that the top of the canopy was captured effectively (TLS: 9.49 m, UAS LiDAR: 9.78 m).

4. Discussion

Canopy fuel properties form a vital component of fire behaviour modelling inputs (Scott, 1999; Finney, 1998, 2006; Van Wagner, 1977; Alexander et al., 2006). To be able to provide such inputs, accurate, quantitative, and spatially explicit representations of different crown fuel elements and their properties are required. Variables such as volume, distance between clumps, and CBH are suitable examples of the types of canopy fuel properties that can be measured using remote sensing technologies. Of course, the accuracy by which these variables can be measured are underpinned by how well different crown fuel elements can be distinguished.

4.1. Automatic separation of canopy fuel and wood in from TLS point clouds

This study has demonstrated the ability of an automated approach to separate crown fuel from wood in TLS and UAS LiDAR point clouds captured in a eucalyptus forest. Prior work has demonstrated the potential to use supervised and unsupervised classification approaches to separate leaf and wood points in point clouds of broadleaf, single stem trees endemic to the northern hemisphere (Li et al., 2018; Ma et al., 2015; Zhu et al., 2018; Vicari et al., 2019; Wang et al., 2018; Krishna et al., 2019). The *TLSeparation* package developed by Vicari (2017) presented a simple, easy to use and flexible approach for use in this manuscript. Whilst the package was originally tested on broadleaf trees, the research presented in this manuscript extended the use of the

Fig. 3. Figures showing a comparison between reference separation and automated separation in TLS and UAS LiDAR point clouds.

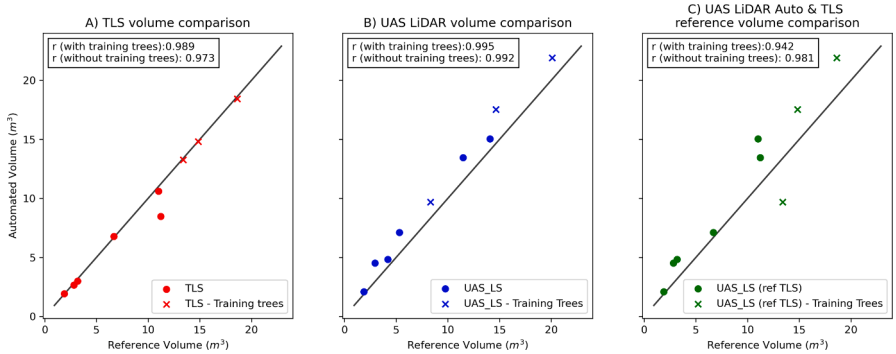

Fig. 4. Figures showing correlation between reference volume and automated volume in T_1 A) TLS point clouds with 0.05 alpha value, B) UAS LiDAR point clouds with 0.15 alpha value and C) UAS LiDAR automated point clouds compared to TLS reference volume.

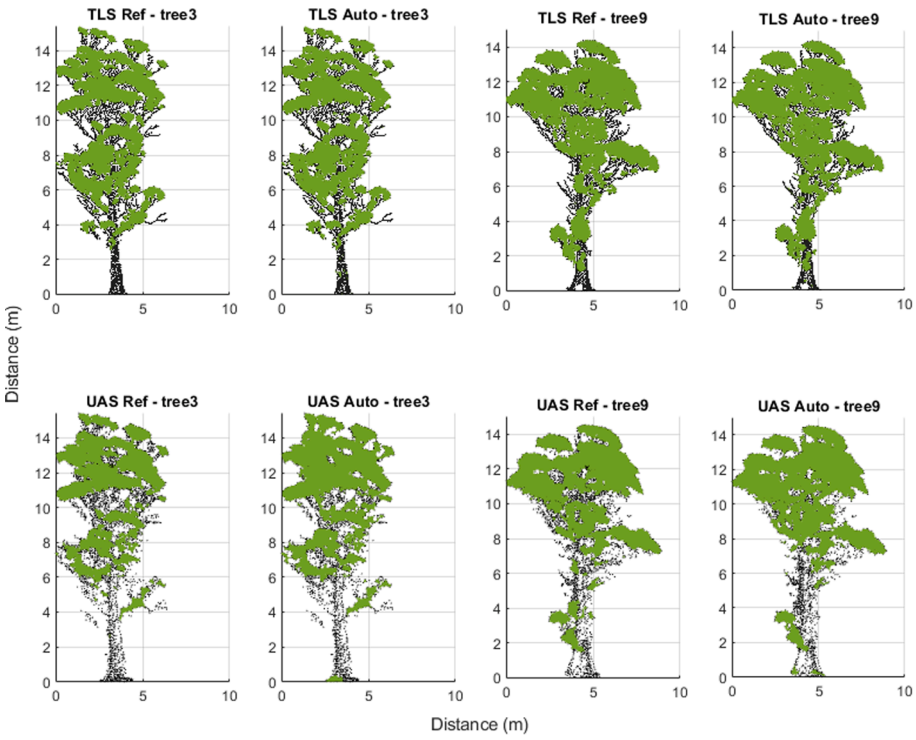

Fig. 5. Volume comparison between TLS and UAS LiDAR point clouds of trees in T_1.

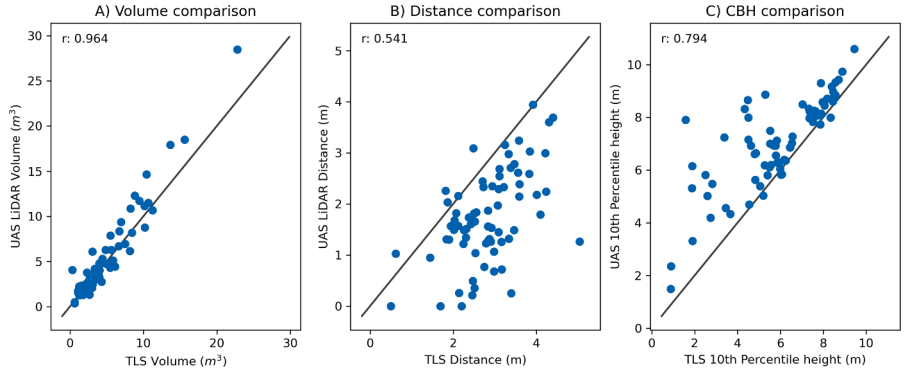

Fig. 6. Figure showing in T_2 A) comparison of average distance between regions in each tree for TLS and UAS LiDAR point clouds; B) comparison between volumes for each tree derived from TLS and UAS LiDAR point clouds and C) comparison between CBH for each tree in TLS and UAS LiDAR point clouds.

package to separate crown fuel and wood points representing eucalypt trees. The eucalypt trees presented unique challenges with the presence of multiple stems, multi-layered canopies, clumped areas of leaves and erectophile leaf angle distribution. The classification of TLS point clouds into the leaf and wood points was achieved with high accuracy (84.6%). Similar accuracy was found by Vicari et al. (2019) in broadleaf trees (83%) and Wang et al. (2020) in tropical trees (91%).

The results achieved here using *TLSeperation*, an unsupervised classifier, are also similar to those achieved using other supervised and unsupervised classification approaches across a range of tree types (Vicari et al., 2019; Wang et al., 2020; Zhu et al., 2018; Ma et al., 2015). Zhu et al. (2018), for instance, used a supervised classifier to achieve classification accuracies above 80 percent. These algorithms utilise and handle different properties (both geometric and intensity based) of the TLS point cloud in order to classify points which could be beneficial for the separation of components of eucalypt trees. As such an area of future research would be to compare the outcomes of methods that consider different combinations of properties within the point cloud (such as Zhu et al. (2018, 2020)).

4.2. Automatic separation of canopy fuel and wood points from UAS LiDAR point clouds

The application of the packages within the *TLSeparation* were also shown to be effective at separating crown fuel and wood points in UAS LiDAR point clouds with overall accuracy of 83.8% and MCC of 0.46. This is a distinct advantage of using a geometric based approach to separate crown fuel and wood which is not reliant on intensity. This is because the UAS LiDAR sensor has a larger footprint which will be partly reflected and therefore make it difficult to distinguish between the materials. The majority (8 of the 9) of reference trees achieved high accuracy (>70%) of separation when compared to manually separated trees. Visual inspection of tree 6, which had poor accuracy (51.5%) and a negative MCC result (−0.06), indicated that this tree had epicormic growth on the trunk with thin protruding branches that had been stripped bare of vegetation. These factors, which also resulted in reduced overall and lower MCC accuracy and an increase in wood omission in TLS point clouds, are amplified in UAS LiDAR with fewer points describing thin parts of the tree. This is consistent with prior

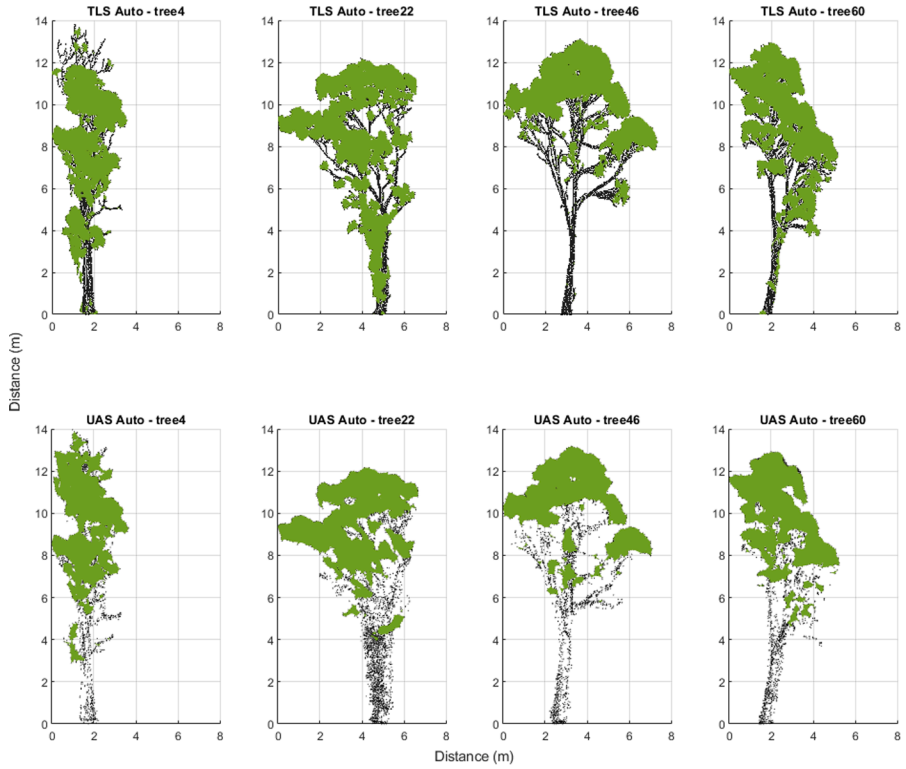

Fig. 7. Visual representation of alpha shapes in the TLS and UAS LiDAR point clouds captured from T_2.

studies which have shown reduced accuracy of modelling the volume of trunks and branches less than 30 cm with UAS LiDAR point clouds (Brede et al., 2019). Further work could investigate the development of crown fuel and wood separation algorithms that are able to generate relevant geometric representations of branches with lower point density. To achieve this high internal geometric precision within the point cloud would be required. In this study a UAS LiDAR system utilising a low precision scanner (due to a large beam divergence and range uncertainty) was used and the separation of points relied on the higher point density offered by UAS systems. Higher grade scanners (either onboard manned or unmanned aircraft) with lower measurement uncertainty would result in point clouds with higher internal precision and improved geometric representations of the trees. When captured at similar pulse densities to those explored in this work the outcome from the UAS LiDAR analysis, either with TLSeparation or alternate algorithms, would likely be enhanced.

4.3. Comparison of TLS and UAS LiDAR sensors

This study also compared the ability of UAS LiDAR and TLS point clouds to estimate crown and canopy fuel properties. An inverse relationship was observed between the TLS and UAS LiDAR point clouds in the respective omission and commission of crown fuel points. In the case of crown fuel points, TLS had a higher percentage of omission and UAS LiDAR had a higher percentage of commission. These differences are likely a function of the algorithm; where visual inspection of the point clouds showed, in the case of the TLS point clouds, that leaves within the canopy were mistakenly classified as wood causing a higher omission in crown fuel and commission in wood points. In contrast, visual inspection of the UAS LiDAR point clouds showed that thin branches were mistakenly classified as crown fuel causing a higher commission of crown fuel and omission of wood points. Despite this, classification accuracies between TLS and UAS LiDAR point clouds were similar (within 0.15 MCC) which led to volume estimates of the crown fuel components derived from the TLS and UAS LiDAR point clouds being highly correlated with reference canopy fuel volumes.

These observations were also evident in T_2 (plot) with strong correlation between TLS and UAS LiDAR volumes at each tree and total volume of the plot. This suggests that despite a reduced accuracy in classification, UAS LiDAR point clouds are still able to detect a suitable number of crown fuel points in each tree to characterise the volume. A negative MBE when predicting canopy fuel volume is consistent with other UAS studies which have shown that UAS LiDAR over predicts the volume of fine scale vegetation (Brede et al., 2019; Madsen et al., 2020). As has been stated in Wallace et al. (2016), the use of a single alpha value likely results in variations in the canopy volume in some regions. Future work should consider the optimisation of the alpha value based on the size of the vegetation elements being observed and the purpose of the assessment. For example, for the determination of canopy volume, consideration of the alpha size should be balanced between the need to represent individual vegetation elements and the likely fire behaviour when fires consume the canopy. That is, the level of convection and radiation are high enough to preheat the fuels such that distance between closely connected fuels is irrelevant.

When analysing crown fuel points within T_2, there were differences in structural attributes observed between TLS and UAS LiDAR point clouds. For points classified as crown fuel in the UAS LiDAR point cloud, a higher mean CTH percentile height was observed in comparison to TLS points classified as crown fuel. This finding is consistent with previous research which found that LiDAR point clouds captured from above the canopy more accurately represented the top most features of the canopy in comparison to TLS which is expected to be due to the viewing perspective (Brede et al., 2017; Hilker et al., 2010; Hillman et al., 2021). Further, by examining the Wilcoxon signed-rank test these differences were shown to be statistically different. Similarly, the ability of each sensor to be able to penetrate and detect the lower regions of the crown were reflected in the CBH which was higher in the UAS LiDAR point clouds and the differences between the CBH estimates of the TLS and UAS LiDAR estimates of CBH to be statistically significantly different. The findings in this study suggest that UAS LiDAR point clouds describe

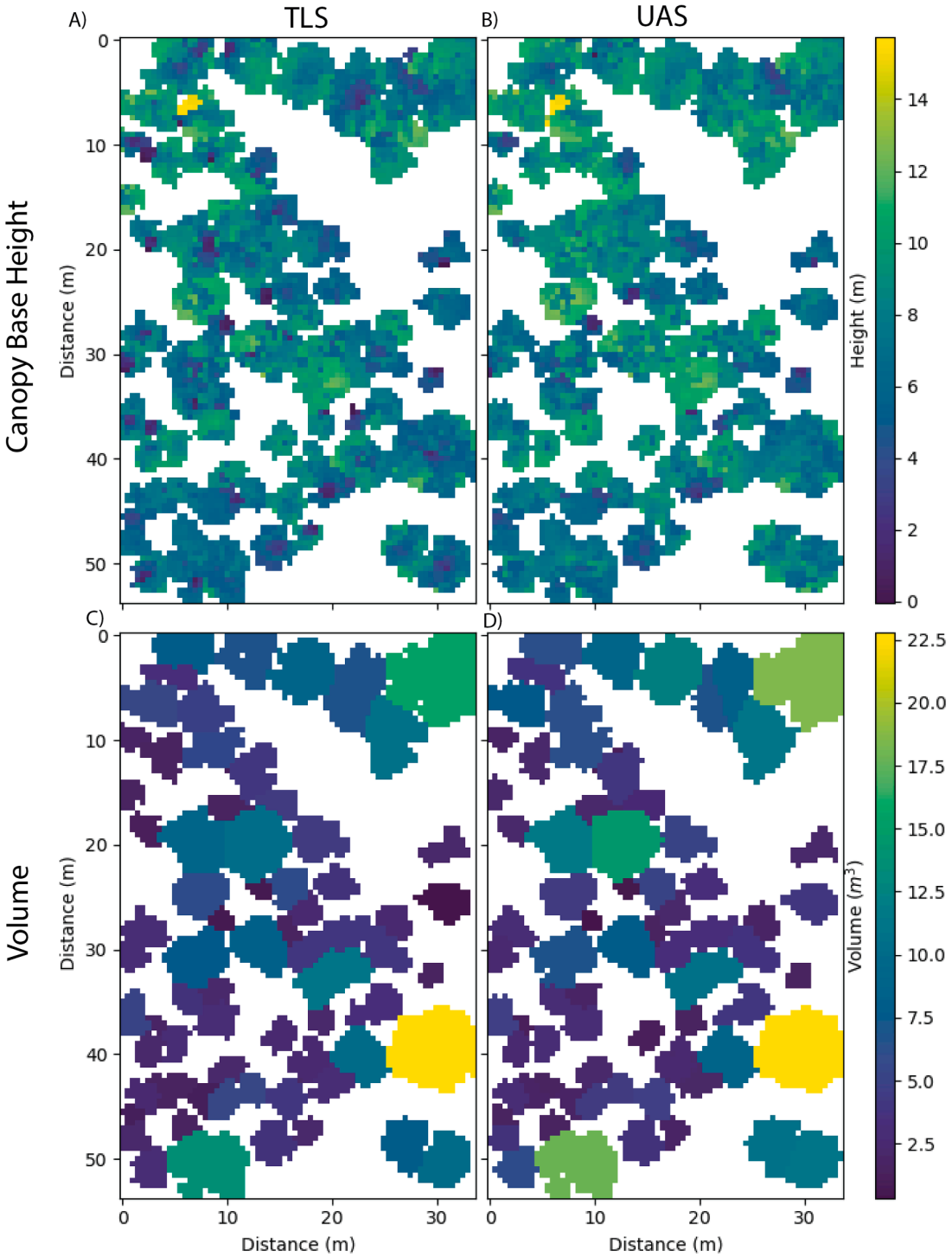

Fig. 8. Comparison of CBH (A and B) and Volume (C and D) of canopy fuel points in TLS and UAS LiDAR point clouds in T_2.

the lower canopy fuel to a lesser extent when compared to TLS. This is supported by prior work Hillman et al. (2021), García et al. (2011), Levick et al. (2021), Brede et al. (2019) which demonstrated the ability of TLS point clouds to provide more information content to describe below canopy vegetation characteristics. More information content within TLS point clouds is also seen in the analysis of the distance between clumps which was shown to be higher in the TLS point clouds than the UAS LiDAR point clouds. This difference is likely a function of the alpha value utilised in the respective point clouds and the ability of UAS LiDAR point clouds to represent lower canopy elements. However, further work should consider the fidelity of the model and consider measuring factors which are relevant to fire behaviour (Duff et al., 2017). That is, a less complete representation of canopy fuel such as that generated from UAS LiDAR point clouds with larger overall clumps may be adequate for representing crown and canopy fuel objects for fire behaviour modelling purposes which may take in broader abstractions of fuel properties (Duff et al., 2017; Gale et al., 2021). The advantage of the TLS point clouds is that they provide a reference for comparison and

potentially a greater level of analysis may be conducted in determining the minimum distance for which objects have to be located apart in order for flaming combustion to occur (Zylstra et al., 2016).

4.4. Operational implications and future research

Separation of fuel elements in the crown enables accurate calculation of fuel properties such as canopy fuel load, canopy bulk density, and fuel strata gap (Cruz et al., 2004; Mitsopoulos and Dimitrakopoulos, 2007). As the capacity of fire behaviour models to ingest new metrics and complex 3D data sets increases, approaches that more directly quantify canopy fuel characteristics may increase model accuracy, compared to the use of simpler regression-derived models of canopy fuel. The approach presented in this manuscript is particularly relevant to eucalyptus forests where there is currently no method to assess the canopy fine fuel characteristics and traditional metrics (e.g. CBH, CFL) may not adequately describe the distributed nature of fuel across the relatively sparse canopy when compared with 'thicker' canopied conifer forests (Price and Gordon, 2016). Additionally, by separating out the stem, it becomes possible to consider the impact and contribution of bark on fuel hazard (Hines et al., 2010; Gould et al., 2008). Whilst not analysed in this work, it is recognised that future approaches should also consider the risk of bark fuels and build on the work mentioned by Pokswinski et al. (2020) in the analysis of fire brands. The accurate separation of fuel and non-fuel objects in the crown leads to potential opportunities to test the algorithm beneath the canopy in the intermediate and elevated fuel layers (Hines et al., 2010). The development of such an approach in combination with the ability to identify vegetation connectivity utilising the methods described in Hillman et al. (2021), Chen et al. (2016) would allow high resolution representation of fuels that contribute to the flaming combustion in the initial passing of a fire. Of note in the application of this approach beneath the canopy is the need to consider the vegetation element size. As highlighted in Vicari et al. (2019), the separation of fine fuels would require the adaption of the current workflow to enable the consideration of the different arrangement of vegetation.

In the future, operational implementation of this research will be aided by improvements and simplifications to processing algorithms, establishing relationships to existing visual based assessments and advancements in sensor-fusion technologies.

Currently data preparation and processing requirements for manual segmentation are time intensive and require expert interpretation. To minimise time required for manual segmentation of trees in the point cloud, fully automated processes such as those presented in Wang et al. (2020) could be trialed or automated tree segmentation algorithms such as those developed in Jaskierniak et al. (2021), Tao et al. (2015b) could be integrated with the *TLSeparation* package (Vicari, 2017), which would simplify the workflow for operational implementation. The data collection and processing of the respective sensors is also important to consider for land managers. Both technologies require expert knowledge to collect and process data with the total time varying due to a number of different factors including but not limited to; vegetation complexity, desired scan density, scanner settings, software and computing resources. Overall it was found that in this case UAS capture and processing was more efficient than the respective TLS workflows. Findings in this study were consistent with Wilkes et al. (2017), Levick et al. (2021), Hillman et al. (2021), who also highlighted that TLS is more time intensive to collect in comparison to UAS which is more efficient data collection process.

Comparing existing visual based assessments and allometric relationships (Skowronski et al., 2011; Duveneck and Patterson, 2007; Keane, 1998; Keane et al., 2000; Botequim et al., 2019) with the canopy fuel metrics derived from algorithms presented in this manuscript is an important piece of future work. This would enable the validation of canopy fuel metrics derived from TLS and UAS LiDAR point clouds in similar forests across the world (Botequim et al., 2019).

Additionally, multi-scale remote sensing derived estimates of canopy fuel properties may potentially be used in conjunction with environmental variables to estimate canopy fuel properties across a broader area (McColl-Gausden et al., 2020). Future research should also focus on the potential to integrate an assessment of vegetation health with the structural separation of crown fuel components allowing for early detection of more flammable material. Research utilising multi-wavelength LIDAR systems which may potentially assist separation algorithms and UAS mounted multi-spectral and hyper-spectral sensors have shown strong overall classification accuracy in identifying declining tree health, bark beetle damage detection and early signs of stress (Danson et al., 2014; Mark Danson et al., 2018; Lehmann et al., 2015; Michez et al., 2016; Näsi et al., 2015; Dash et al., 2017). Overall, by accurately separating crown fuels and assessing canopy fuel properties at high resolution a potential paradigm shift is made possible in the way land managers are able to estimate fuel risk and predict the behaviour of fires.

5. Conclusions

Next-generation fire simulations provide unique opportunities for the fire community to produce metrics that are driven by fundamental fire behaviour. It is therefore important to investigate the potential of high resolution point clouds to represent fuel objects which are likely to be consumed in the initial passing of fire. This study demonstrates that crown fuel and wood points can be separated in TLS and UAS LiDAR point clouds to determine canopy fuel properties of eucalyptus trees. Results from the study demonstrate that TLS and UAS LiDAR point clouds were able to accurately classify crown fuel and wood points when compared to manually separated point clouds as reference data. TLS point clouds were shown to provide the most accurate form of separation with thin branch diameter, epicormic growth and lower information content in UAS LiDAR point clouds impacting the accuracy of the calculation on some reference trees. Despite differences in the accuracy of classification of crown and woody fuel, crown volume estimates from automatically separated TLS and UAS LiDAR point clouds were highly correlated with volume estimates derived from reference trees. When scaled up to the plot, strong correlation between UAS LiDAR and TLS point cloud canopy volumes was observed. TLS point clouds were shown to represent the bottom of the canopy and information within the canopy itself to a greater extent than UAS LiDAR as shown by a lower mean CBH and greater distance between clumps at the plot scale. This increased information content provided in the TLS point clouds should be balanced against the ability of fire behaviour modelling to utilise the increased information contained within these point clouds. Overall, this study demonstrates that separation of crown fuel and wood in eucalyptus forests is operationally achievable and represents a unique opportunity for the accurate derivation of canopy fuel properties. Further exploration in the application of this methodology to separate fuel beneath the canopy and sensor fusion, has the potential to enable a paradigm shift in the way fuels are estimated that is commensurate with fire simulation developments and requirements.

Declaration of Competing Interest

The authors declare that they have no known competing financial interests or personal relationships that could have appeared to influence the work reported in this paper.

Acknowledgement

The support of the Commonwealth of Australia through the Bushfire and Natural Hazards Cooperative Research Centre and the Australian Postgraduate Award is acknowledged. Bryan Hally and Ahmad Fallatah are acknowledged for assistance in the collection of the data. The University of Tasmania specifically Arko Lucieer and Darren Turner, are

gratefully acknowledged for providing their equipment, lab and expertise.

This research was funded by Bushfire Natural Hazard CRC(CON/2017/01377).

References

Aijazi, A.K., Checchin, P., Trassoudaine, L., 2013. Detecting and Updating Changes in Lidar Point Clouds for Automatic 3D Urban Cartography. ISPRS Ann. Photogramm. Remote Sens. Spatial Inform. Sci. 2 (5W2), 7–12. https://doi.org/10.5194/isprsannals-II-5-W2-7-2013. ISSN 21949050.

Alexander, Martin E., Cruz, Miguel G., Lopes, A.M.G., 2006. Cfis: a software tool for simulating crown fire initiation and spread. For. Ecol. Manage. 234 (1), S133.

Andersen, Hans-Erik, McGaughey, Robert J., Reutebuch, Stephen E., 2005. Estimating forest canopy fuel parameters using lidar data. Remote Sens. Environ. 94 (4), 441–449.

Béland, Martin, Baldocchi, Dennis D., Widlowski, Jean-Luc, Fournier, Richard A., Verstraete, Michel M., 2014. On seeing the wood from the leaves and the role of voxel size in determining leaf area distribution of forests with terrestrial lidar. Agric. For. Meteorol. 184, 82–97.

Botequim, Brigite, Fernandes, Paulo M., Borges, José G., González-Ferreiro, Eduardo, Guerra-Hernández, Juan, 2019. Improving silvicultural practices for mediterranean forests through fire behaviour modelling using lidar-derived canopy fuel characteristics. Int. J. Wildland Fire 28 (11), 823–839.

Boughorbel, Sabri, Jarray, Fethi, El-Anbari, Mohammed, 2017. Optimal classifier for imbalanced data using Matthews Correlation Coefficient metric. PLoS ONE 12 (6), 1–ss-17. https://doi.org/10.1371/journal.pone.0177678. ISSN 19326203.

Brede, Benjamin, Lau, Alvaro, Bartholomeus, Harm M., Kooistra, Lammert, 2017. Comparing riegl ricopter uav lidar derived canopy height and dbh with terrestrial lidar. Sensors 17 (10), 2371.

Brede, Benjamin, Calders, Kim, Lau, Alvaro, Raumonen, Pasi, Bartholomeus, Harm M, Herold, Martin, Kooistra, Lammert, 2019. Non-destructive tree volume estimation through quantitative structure modelling: Comparing uav laser scanning with terrestrial lidar. Remote Sens. Environ. 233, 111355.

Calders, Kim, Newnham, Glenn, Burt, Andrew, Murphy, Simon, Raumonen, Pasi, Herold, Martin, Culvenor, Darius, Avitabile, Valerio, Disney, Mathias, Armston, John, et al., 2015. Nondestructive estimates of above-ground biomass using terrestrial laser scanning. Methods Ecol. Evol. 6 (2), 198–208.

Camarretta, Nicolò, Harrison, Peter A., Lucieer, Arko, Potts, Brad M., Davidson, Neil, Hunt, Mark, 2020. From drones to phenotype: Using uav-lidar to detect species and provenance variation in tree productivity and structure. Remote Sens. 12 (19), 3184.

Cao, Lin, Coops, Nicholas C., Hermosilla, Txomin, Innes, John, Dai, Jinsong, She, Guanghui, 2014. Using small-footprint discrete and full-waveform airborne lidar metrics to estimate total biomass and biomass components in subtropical forests. Remote Sens. 6 (8), 7110–7135.

Cao, Lin, Liu, Hao, Xiaoyao, Fu., Zhang, Zhengnan, Shen, Xin, Ruan, Honghua, 2019. Comparison of uav lidar and digital aerial photogrammetry point clouds for estimating forest structural attributes in subtropical planted forests. Forests 10 (2), 145.

Chen, Yang, Zhu, Xuan, Yebra, Marta, Harris, Sarah, Tapper, Nigel, 2016. Strata-based forest fuel classification for wild fire hazard assessment using terrestrial lidar. J. Appl. Remote Sens. 10 (4), 046025.

Cruz, Miguel G., Alexander, Martin E., 2013. Uncertainty associated with model predictions of surface and crown fire rates of spread. Environ. Model. Softw. 47, 16–28.

Cruz, Miguel G., Alexander, Martin E., Wakimoto, Ronald H., 2004. Modeling the likelihood of crown fire occurrence in conifer forest stands. For. Sci. 50 (5), 640–658.

Cruz, Miguel G, Lachie McCaw, W., Anderson, Wendy R., Gould, Jim S., 2013. Fire behaviour modelling in semi-arid mallee-heath shrublands of southern australia. Environ. Model. Softw. 40, 21–34.

Danson, F. Mark, Gaulton, Rachel, Armitage, Richard P., Disney, Mathias, Gunawan, Oliver, Lewis, Philip, Pearson, Guy, Ramirez, Alberto F., 2014. Developing a dual-wavelength full-waveform terrestrial laser scanner to characterize forest canopy structure. Agric. For. Meteorol. 198, 7–14.

Dash, Jonathan P., Watt, Michael S., Pearse, Grant D., Heaphy, Marie, Dungey, Heidi S., 2017. Assessing very high resolution uav imagery for monitoring forest health during a simulated disease outbreak. ISPRS J. Photogramm. Remote Sens. 131, 1–14.

Disney, M., Burt, A., Calders, Kim, Schaaf, C., Stovall, A., 2019. Innovations in ground and airborne technologies as reference and for training and validation: terrestrial laser scanning (tls). Surv. Geophys. 1–22.

du Toit, Francois, Coops, Nicholas C., Tompalski, Piotr, Goodbody, Tristan R.H., El-Kassaby, Yousry A., Stoehr, Michael, Turner, Darren, Lucieer, Arko, 2020. Characterizing variations in growth characteristics between douglas-fir with different genetic gain levels using airborne laser scanning. Trees 1–16.

Duff, Thomas J., Keane, Robert E., Penman, Trent D., Tolhurst, Kevin G., 2017. Revisiting wildland fire fuel quantification methods: the challenge of understanding a dynamic, biotic entity. Forests 8 (9), 351.

Duveneck, Matthew J., Patterson III, William A., 2007. Characterizing canopy fuels to predict fire behavior in pitch pine stands. Northern J. Appl. Forestry 24 (1), 65–70.

Edelsbrunner, Herbert, Mücke, Ernst P., 1994. Three-dimensional alpha shapes. ACM Trans. Graph. (TOG) 13 (1), 43–72.

Engelstad, Peder S., Falkowski, Michael, Wolter, Peter, Poznanovic, Aaron, Johnson, Patty, 2019. Estimating canopy fuel attributes from low-density lidar. Fire 2 (3), 38.

Finney, Mark A., 1998. FARSITE, Fire Area Simulator–model development and evaluation. Number 4. US Department of Agriculture, Forest Service, Rocky Mountain Research Station.

Finney, Mark A, 2006. An overview of flammap fire modeling capabilities. In: Andrews, Patricia L., Butler, Bret W. (Eds.), comps. 2006. Fuels Management-How to Measure Success: Conference Proceedings. 28–30 March 2006; Portland, OR. Proceedings RMRS-P-41. Fort Collins, CO: US Department of Agriculture, Forest Service, Rocky Mountain Research Station, vol. 41. p. 213–220.

Fritz, Andreas, Kattenborn, Teja, Koch, B., 2013. Uav-based photogrammetric point clouds–tree stem mapping in open stands in comparison to terrestrial laser scanner point clouds. Int. Arch. Photogramm. Remote Sens. Spat. Inf. Sci 40, 141–146.

Gale, Matthew G., Cary, Geoffrey J., Van Dijk, Albert I.J.M., Yebra, Marta, 2021. Forest fire fuel through the lens of remote sensing: Review of approaches, challenges and future directions in the remote sensing of biotic determinants of fire behaviour. Remote Sens. Environ. 255, 112282.

García, Mariano, Danson, F. Mark, Riano, David, Chuvieco, Emilio, Ramirez, F. Alberto, Bandugula, Vishal, 2011. Terrestrial laser scanning to estimate plot-level forest canopy fuel properties. Int. J. Appl. Earth Observ. Geoinform. 13 (4), 636–645.

Gawel, Abel, Cieslewski, Titus, Dubé, Renaud, Bosse, Mike, Siegwart, Roland, Nieto, Juan, 2016. Structure-based vision-laser matching. In: IEEE International Conference on Intelligent Robots and Systems, 2016-Novem:182–188, 2016. doi: 10.1109/IROS.2016.7759053. ISSN 21530866.

Gazzard, Tim, Walshe, Terry, Galvin, Peter, Salkin, Owen, Baker, Michael, Cross, Bec, Ashton, Peter, 2020. What is the 'appropriate'fuel management regime for the otway ranges, victoria, australia? developing a long-term fuel management strategy using the structured decision-making framework. Int. J. Wildland Fire 29 (5), 354–370.

Girardeau-Montaut, Daniel, 2016. Cloudcompare. Retrieved from CloudCompare: https://www.danielgm.net/cc.

González-Olabarria, José-Ramón, Rodríguez, Francisco, Fernández-Landa, Alfredo, Mola-Yudego, Blas, 2012. Mapping fire risk in the model forest of urbión (spain) based on airborne lidar measurements. For. Ecol. Manage. 282, 149–156.

Gorte, Ross, Economics, Headwater, 2013. The rising cost of wildfire protection. Headwaters Economics Bozeman, MT.

Gould, James Stanley, McCaw, W.L., Cheney, N.P., Ellis, P.F., Knight, I.K., Sullivan, A.L., 2008. Project Vesta: fire in dry eucalypt forest: fuel structure, fuel dynamics and fire behaviour. Csiro Publishing.

Grubinger, Samuel, Coops, Nicholas C., Stoehr, Michael, El-Kassaby, Yousry A., Lucieer, Arko, Turner, Darren, 2020. Modeling realized gains in douglas-fir (pseudotsuga menziesii) using laser scanning data from unmanned aircraft systems (uas). For. Ecol. Manage. 473, 118284.

Guerra-Hernández, J., Tomé, Margarida, González-Ferreiro, E., 2016. Using low density lidar data to map mediterranean forest characteristics by means of an area-based approach and height threshold analysis. Revista de Teledetección (46), 103–117.

Guo, Qinghua, Su, Yanjun, Hu, Tianyu, Zhao, Xiaoqian, Wu, Fangfang, Li, Yumei, Liu, Jin, Chen, Linhai, Guangcai, Xu., Lin, Guanghui, et al., 2017. An integrated uav-borne lidar system for 3d habitat mapping in three forest ecosystems across china. Int. J. Remote Sens. 38 (8–10), 2954–2972.

Hall, S.A., Burke, I.C., Box, D.O., Kaufmann, M.R., Stoker, Jason M., 2005. Estimating stand structure using discrete-return lidar: an example from low density, fire prone ponderosa pine forests. For. Ecol. Manage. 208 (1–3), 189–209.

Hermosilla, Txomin, Ruiz, Luis A., Kazakova, Alexandra N., Coops, Nicholas C., Moskal, L. Monika, 2014. Estimation of forest structure and canopy fuel parameters from small-footprint full-waveform lidar data. Int. J. Wildland Fire 23 (2), 224–233.

Hilker, Thomas, van Leeuwen, Martin, Coops, Nicholas C., Wulder, Michael A., Newnham, Glenn J., Jupp, David L.B., Culvenor, Darius S., 2010. Comparing canopy metrics derived from terrestrial and airborne laser scanning in a douglas-fir dominated forest stand. Trees 24 (5), 819–832.

Hillman, Samuel, Wallace, Luke, Reinke, Karin, Hally, Bryan, Jones, Simon, Saldias, Daisy S., 2019. A method for validating the structural completeness of understory vegetation models captured with 3d remote sensing. Remote Sens. 11 (18), 2118.

Hillman, Samuel, Wallace, Luke, Lucieer, Arko, Reinke, Karin, Turner, Darren, Jones, Simon, 2021. A comparison of terrestrial and UAS sensors for measuring fuel hazard in a dry sclerophyll forest. Int. J. Appl. Earth Observ. Geoinform. 95(October 2020), 102261. doi: 10.1016/j.jag.2020.102261. http://www.sciencedirect.com/science/article/pii/S0303243420309041. ISSN 0303-2434.

Hines, Francis, Tolhurst, Kevin G., Wilson, Andrew A.G., McCarthy, Gregory J., 2010. Overall fuel hazard assessment guide. Number 82. Victorian Government, Department of Sustainability and Environment. ISBN 9781742426761.

Jaskierniak, D., Lucieer, A., Kuczera, G., Turner, D., Lane, P.N.J., Benyon, R.G., Haydon, S., 2021. Individual tree detection and crown delineation from unmanned aircraft system (uas) lidar in structurally complex mixed species eucalypt forests. ISPRS J. Photogramm. Remote Sens. 171, 171–187.

Keane, Robert E., 1998. Development of input data layers for the FARSITE fire growth model for the Selway-Bitterroot Wilderness complex, USA, vol. 3. US Department of Agriculture, Forest Service, Rocky Mountain Research Station.

Keane, Robert E., Mincemoyer, Scott A., Schmidt, Kirsten M., Long, Donald G., Garner, Janice L., 2000. Mapping vegetation and fuels for fire management on the gila national forest complex, new mexico. Gen. Tech. Rep. RMRS-GTR-46, vol. 126. US Department of Agriculture, Forest Service, Rocky Mountain Research Station, Ogden, UT, p. 46.

Latifi, Hooman, Heurich, Marco, Hartig, Florian, Müller, Jörg, Krzystek, Peter, Jehl, Hans, Dech, Stefan, 2016. Estimating over-and understorey canopy density of temperate mixed stands by airborne lidar data. For. Int. J. For. Res. 89 (1), 69–81.

Lee, Alex C., Lucas, Richard M., 2007. A lidar-derived canopy density model for tree stem and crown mapping in australian forests. Remote Sens. Environ. 111 (4), 493–518.

Lehmann, Jan Rudolf Karl, Nieberding, Felix, Prinz, Torsten, Knoth, Christian, 2015. Analysis of unmanned aerial system-based cir images in forestry–a new perspective to monitor pest infestation levels. Forests 6 (3), 594–612.
Levick, Shaun R., Whiteside, Tim, Loewensteiner, David A., Rudge, Mitchel, Bartolo, Renee, 2021. Leveraging tls as a calibration and validation tool for mls and uls mapping of savanna structure and biomass at landscape-scales. Remote Sens. 13 (2), 257.
Li, Zhan, Schaefer, Michael, Strahler, Alan, Schaaf, Crystal, Jupp, David, 2018. On the utilization of novel spectral laser scanning for three-dimensional classification of vegetation elements. Interface Focus 8 (2), 20170039.
Liu, Kun, Shen, Xin, Cao, Lin, Wang, Guibin, Cao, Fuliang, 2018. The evaluation of parametric and non-parametric models for total forest biomass estimation using uas-lidar. In: 2018 Fifth International Workshop on Earth Observation and Remote Sensing Applications (EORSA). IEEE, pp. 1–5.
Ma, Lixia, Zheng, Guang, Eitel, Jan U.H., Moskal, L. Monika, He, Wei, Huang, Huabing, 2015. Improved salient feature-based approach for automatically separating photosynthetic and nonphotosynthetic components within terrestrial lidar point cloud data of forest canopies. IEEE Trans. Geosci. Remote Sens. 54 (2), 679–696.
Madsen, Bjarke, Treier, Urs A., Zlinszky, András, Lucieer, Arko, Normand, Signe, 2020. Detecting shrub encroachment in seminatural grasslands using uas lidar. Ecol. Evol. 10 (11), 4876–4902.
Mark Danson, F., Sasse, Fadal, Schofield, Lucy A., 2018. Spectral and spatial information from a novel dual-wavelength full-waveform terrestrial laser scanner for forest ecology. Interface Focus 8 (2), 20170049.
McColl-Gausden, S.C., Bennett, L.T., Duff, T.J., Cawson, J.G., Penman, T.D., 2020. Climatic and edaphic gradients predict variation in wildland fuel hazard in south-eastern australia. Ecography 43 (3), 443–455.
Michez, Adrien, Piégay, Hervé, Lisein, Jonathan, Claessens, Hugues, Lejeune, Philippe, 2016. Classification of riparian forest species and health condition using multi-temporal and hyperspatial imagery from unmanned aerial system. Environ. Monit. Assessm. 188 (3), 146.
Mitsopoulos, Ioannis D., Dimitrakopoulos, Alexandros P., 2007. Canopy fuel characteristics and potential crown fire behavior in aleppo pine (pinus halepensis mill.) forests. Ann. For. Sci. 64 (3), 287–299.
Krishna, Sruthi M., Moorthy, Kim Calders, Vicari, Matheus B., Verbeeck, Hans, 2019. Improved supervised learning-based approach for leaf and wood classification from lidar point clouds of forests. IEEE Trans. Geosci. Remote Sens. 58 (5), 3057–3070.
Näsi, Roope, Honkavaara, Eija, Lyytikäinen-Saarenmaa, Päivi, Blomqvist, Minna, Litkey, Paula, Hakala, Teemu, Viljanen, Niko, Kantola, Tuula, Tanhuanpää, Topi, Holopainen, Markus, 2015. Using uav-based photogrammetry and hyperspectral imaging for mapping bark beetle damage at tree-level. Remote Sens. 7 (11), 15467–15493.
Newnham, Glenn J., Armston, John D., Calders, Kim, Disney, Mathias I., Lovell, Jenny L., Schaaf, Crystal B., Strahler, Alan H., Mark Danson, F., 2015. Terrestrial Laser Scanning for Plot-Scale Forest Measurement. Curr. For. Rep. 1(4), 239–251. doi: 10.1007/s40725-015-0025-5. ISSN 2198-6436.
Patenaude, Genevieve, Milne, Ronald, Dawson, Terence P., 2005. Synthesis of remote sensing approaches for forest carbon estimation: reporting to the kyoto protocol. Environ. Sci. Policy 8 (2), 161–178.
Peng, Xi, Zhao, Anjiu, Chen, Yongfu, Chen, Qiao, Liu, Haodong, Wang, Juan, Li, Huayu, 2020. Comparison of modeling algorithms for forest canopy structures based on uav-lidar: A case study in tropical china. Forests 11 (12), 1324.
Penman, T.D., Cirulis, B.A., 2020. Cost effectiveness of fire management strategies in southern australia. Int. J. Wildland Fire 29 (5), 427–439.
Pokswinski, Scott, Gallagher, Michael R., Skowronski, Nicholas S., Louise Loudermilk, E., O'Brien, Joseph J., Kevin Hiers, J., 2020. Diurnal pine bark structure dynamics affect properties relevant to firebrand generation. Fire 3(4), 55.
Price, Owen F., Gordon, Christopher E., 2016. The potential for lidar technology to map fire fuel hazard over large areas of australian forest. J. Environ. Manage. 181, 663–673.
Romero Ramirez, Francisco J., Navarro-Cerrillo, Rafael Ma, Varo-Martínez, Ma Ángeles, Quero, Jose Luis, Doerr, Stefan, Hernández-Clemente, Rocío, 2018. Determination of forest fuels characteristics in mortality-affected pinus forests using integrated hyperspectral and als data. Int. J. Appl. Earth Observ. Geoinform. 68, 157–167.
Raymond, Crystal L., Peterson, David L., 2005. Fuel treatments alter the effects of wildfire in a mixed-evergreen forest, Oregon, USA. Can. J. For. Res. 35 (12), 2981–2995.
Rothermel, Richard C., 1986. Modeling moisture content of fine dead wildland fuels: input to the BEHAVE fire prediction system. US Department of Agriculture, Forest Service, Intermountain Research Station, USA.
Rowell, E. Eric, Loudermilk, Louise, Seielstad, Carl, O'Brien, Joseph J, 2016. Using simulated 3d surface fuelbeds and terrestrial laser scan data to develop inputs to fire behavior models. Can. J. Remote Sens. 42 (5), 443–459.
Sankey, Temuulen, Donager, Jonathon, McVay, Jason, Sankey, Joel B, 2017. Uav lidar and hyperspectral fusion for forest monitoring in the southwestern USA. Remote Sens. Environ. 195, 30–43.
Scott, Joe H., 1999. Nexus: a system for assessing crown fire hazard. Fire Manage. Notes.
Scott, Joe H., 2005. Standard fire behavior fuel models: a comprehensive set for use with Rothermel's surface fire spread model. US Department of Agriculture, Forest Service, Rocky Mountain Research Station.
Skowronski, Nicholas, Clark, Kenneth, Nelson, Ross, Hom, John, Patterson, Matt, 2007. Remotely sensed measurements of forest structure and fuel loads in the pinelands of new jersey. Remote Sens. Environ. 108 (2), 123–129.
Skowronski, Nicholas S., Clark, Kenneth L., Duveneck, Matthew, Hom, John, 2011. Three-dimensional canopy fuel loading predicted using upward and downward sensing lidar systems. Remote Sens. Environ. 115 (2), 703–714.
Sullivan, Andrew L., Lachie McCaw, W., Cruz, Miguel G., Matthews, Stuart, Ellis, Peter F., 2012. Fuel, fire weather and fire behaviour in australian ecosystems. Flammable Australia: fire regimes, biodiversity and ecosystems in a changing world, pp. 51–77.
Tao, Shengli, Guo, Qinghua, Shiwu, Xu., Yanjun, Su., Li, Yumei, Fangfang, Wu., 2015a. A geometric method for wood-leaf separation using terrestrial and simulated lidar data. Photogramm. Eng. Remote Sens. 81 (10), 767–776.
Tao, Shengli, Fangfang, Wu., Guo, Qinghua, Wang, Yongcai, Li, Wenkai, Xue, Baolin, Xueyang, Hu., Li, Peng, Tian, Di, Li, Chao, et al., 2015b. Segmenting tree crowns from terrestrial and mobile lidar data by exploring ecological theories. ISPRS J. Photogramm. Remote Sens. 110, 66–76.
Vicari, M., 2018. Tlseparation. https://tlseparation.github.io/documentation/index.html.
Vicari, Matheus B., Disney, Mathias, Wilkes, Phil, Burt, Andrew, Calders, Kim, Woodgate, William, 2019. Leaf and wood classification framework for terrestrial lidar point clouds. Methods Ecol. Evol. 10 (5), 680–694.
Viney, Neil R., 1991. A review of fine fuel moisture modelling. Int. J. Wildland Fire 1 (4), 215–234.
Van Wagner, C.E., 1977. Conditions for the start and spread of crown fire. Can. J. For. Res. 7 (1), 23–34.
Wallace, Luke, Lucieer, Arko, Watson, Christopher, Turner, Darren, 2012. Development of a uav-lidar system with application to forest inventory. Remote Sens. 4 (6), 1519–1543.
Wallace, Luke, Musk, Robert, Lucieer, Arko, 2014a. An assessment of the repeatability of automatic forest inventory metrics derived from UAV-borne laser scanning data. IEEE Trans. Geosci. Remote Sens. 52 (11), 7160–7169. https://doi.org/10.1109/TGRS.2014.2308208. ISSN 01962892.
Wallace, Luke, Watson, Christopher, Lucieer, Arko, 2014b. Detecting pruning of individual stems using airborne laser scanning data captured from an unmanned aerial vehicle. Int. J. Appl. Earth Obs. Geoinf. 30, 76–85.
Wallace, Luke, Lucieer, Arko, Malenovský, Zbyněk, Turner, Darren, Vopěnka, Petr, 2016. Assessment of forest structure using two uav techniques: A comparison of airborne laser scanning and structure from motion (sfm) point clouds. Forests 7 (3), 62.
Wang, Di, 2020. Unsupervised semantic and instance segmentation of forest point clouds. ISPRS J. Photogramm. Remote Sens. 165, 86–97.
Wang, Di, Brunner, Jasmin, Ma, Zhenyu, Hao, Lu., Hollaus, Markus, Pang, Yong, Pfeifer, Norbert, 2018. Separating tree photosynthetic and non-photosynthetic components from point cloud data using dynamic segment merging. Forests 9 (5), 252.
Wang, Di, Takoudjou, Stéphane Momo, Casella, Eric, 2020. Lewos: A universal leaf-wood classification method to facilitate the 3d modelling of large tropical trees using terrestrial lidar. Methods Ecol. Evol. 11 (3), 376–389.
Wang, Zhen, Zhang, Liqiang, Fang, Tian, Mathiopoulos, P. Takis, Tong, Xiaohua, Qu, Huamin, Xiao, Zhiqiang, Li, Fang, Chen, Dong, 2014. A multiscale and hierarchical feature extraction method for terrestrial laser scanning point cloud classification. IEEE Trans. Geosci. Remote Sens. 53(5), 2409–2425.
Wieser, Martin, Mandlburger, Gottfried, Hollaus, Markus, Otepka, Johannes, Glira, Philipp, Pfeifer, Norbert, 2017. A case study of uas borne laser scanning for measurement of tree stem diameter. Remote Sens. 9 (11), 1154.
Wilkes, Phil, Lau, Alvaro, Disney, Mathias I., Calders, Kim, Burt, Andrew, 2017. Data Acquisition Considerations for Terrestrial Laser Scanning of Forest Plots. Remote Sens. Environ. 196 (May), 140–153. https://doi.org/10.1016/j.rse.2017.04.030. ISSN 00344257, URL https://doi.org/10.1016/j.rse.2017.04.030.
Wu, Bingxiao, Zheng, Guang, Chen, Yang, 2020. An improved convolution neural network-based model for classifying foliage and woody components from terrestrial laser scanning data. Remote Sens. 12 (6), 1010.
Wulder, Michael A., Seemann, David, 2003. Forest inventory height update through the integration of lidar data with segmented landsat imagery. Can. J. Remote Sens. 29 (5), 536–543.
Zhao, Kaiguang, Popescu, Sorin, Meng, Xuelian, Pang, Yong, Agca, Muge, 2011. Characterizing forest canopy structure with lidar composite metrics and machine learning. Remote Sens. Environ. 115 (8), 1978–1996.
Zhu, Xi, Skidmore, Andrew K., Darvishzadeh, Roshanak, Olaf Niemann, K., Liu, Jing, Shi, Yifang, Wang, Tiejun, 2018. Foliar and woody materials discriminated using terrestrial lidar in a mixed natural forest. Int. J. Appl. Earth Observ. Geoinform. 64, 43–50.
Zylstra, Philip, Bradstock, Ross A., Bedward, Michael, Penman, Trent D., Doherty, Michael D., Weber, Rodney O., Malcolm Gill, A., Cary, Geoffrey J., 2016. Biophysical mechanistic modelling quantifies the effects of plant traits on fire severity: species, not surface fuel loads, determine flame dimensions in eucalypt forests. PloS One 11 (8), e0160715.